



This is a repository copy of *A review of flow control for gust load alleviation*.

White Rose Research Online URL for this paper:

<https://eprints.whiterose.ac.uk/193050/>

Version: Published Version

Article:

Li, Y. and Qin, N. orcid.org/0000-0002-6437-9027 (2022) A review of flow control for gust load alleviation. *Applied Sciences*, 12 (20). 10537. ISSN 2076-3417

<https://doi.org/10.3390/app122010537>

Reuse

This article is distributed under the terms of the Creative Commons Attribution (CC BY) licence. This licence allows you to distribute, remix, tweak, and build upon the work, even commercially, as long as you credit the authors for the original work. More information and the full terms of the licence here:

<https://creativecommons.org/licenses/>

Takedown

If you consider content in White Rose Research Online to be in breach of UK law, please notify us by emailing eprints@whiterose.ac.uk including the URL of the record and the reason for the withdrawal request.



eprints@whiterose.ac.uk
<https://eprints.whiterose.ac.uk/>

Review

A Review of Flow Control for Gust Load Alleviation

Yonghong Li ^{1,2} and Ning Qin ^{1,*}¹ Department of Mechanical Engineering, The University of Sheffield, Sheffield S1 3JD, UK² High Speed Aerodynamic Institute, China Aerodynamic Research and Development Center, Mianyang 621000, China

* Correspondence: n.qin@sheffield.ac.uk

Featured Application: Gust load control, aircraft weight reduction, aircraft drag reduction.

Abstract: Effective control of aerodynamic loads, such as maneuvering load and gust load, allows for reduced structural weight and therefore greater aerodynamic efficiency. After a basic introduction in the types of gusts and the current gust load control strategies for aircraft, we outline the conventional gust load alleviation techniques using trailing-edge flaps and spoilers. As these devices also function as high-lift devices or inflight speed brakes, they are often too heavy for high-frequency activations such as control surfaces. Non-conventional active control devices via fluidic actuators have attracted some attention recently from researchers to explore more effective gust load alleviation techniques against traditional flaps for future aircraft design. Research progress of flow control using fluidic actuators, including surface jet blowing and circulation control (CC) for gust load alleviation, is reviewed in detail here. Their load control capabilities in terms of lift force modulations are outlined and compared. Also reviewed are the flow control performances of these fluidic actuators under gust conditions. Experiments and numerical efforts indicated that both CC and surface jet blowing demonstrate fast response characteristics, capable for timely adaptive gust load controls.

Keywords: gust load alleviation; active flow control; blowing jet control; circulation control

Citation: Li, Y.; Qin, N. A Review of Flow Control for Gust Load Alleviation. *Appl. Sci.* **2022**, *12*, 10537. <https://doi.org/10.3390/app122010537>

Academic Editor: Josep Maria Bergada

Received: 26 September 2022

Accepted: 17 October 2022

Published: 19 October 2022

Publisher's Note: MDPI stays neutral with regard to jurisdictional claims in published maps and institutional affiliations.



Copyright: © 2022 by the authors. Licensee MDPI, Basel, Switzerland. This article is an open access article distributed under the terms and conditions of the Creative Commons Attribution (CC BY) license (<https://creativecommons.org/licenses/by/4.0/>).

1. Introduction

It is undeniable that air travel makes fast long-distance transportation possible and brings significant economic growth and improvement of quality of life. However, in the meantime, the negative impacts on the environment and climate [1] have become more and more pronounced and have posed a significant challenge to the aviation industry. For economic and ecological considerations, reduction in fuel consumption and exhaust emissions is very urgent task for future air transportation. For this purpose, the aviation industry is facing stringent 'Green Aviation' goals in their future product. For example, the primary goal of Europe's Flight-path 2050 is to reduce CO₂ emissions of aircraft by 75% relative to 2005 levels [2]. In the US, the N+3 goal proposed by NASA is to reduce Nitrogen oxides (NO_x) emission by up to 80% in the landing-take-off process and reduce fuel burn by 60% for an airliner entering service in 2030–2035 [3]. To achieve these objectives, a number of technologies, such as shock control [4–7], laminar flow control [8–14], turbulent drag reduction [15–18], as well as novel aircraft concepts, such as BWB or hybrid wing body (HWB) [19], 'double-bubble' [20], truss-braced wing (TBW) [21] and box-wing [22], have been proposed and investigated to explore a better aerodynamic performance. However, there are significant challenges in applying these technologies mentioned above on future aircraft, especially in terms of practical application. Meanwhile, with the increasing development and maturity in computational fluid dynamics (CFD) and aerodynamic design optimization, the aerodynamic efficiency of modern swept supercritical wings has almost reached its limit with diminishing return from large research investment. Therefore, it is urgent to explore game-changing technologies for drag reduction associated with the

reduction in exhaust emissions. Load control is an important topic in aerodynamics, as it can potentially provide an alternative way for drag reduction through decreasing the aircraft structure weight. Figure 1 shows the relationship among flow control, load control, aerodynamic performance and energy efficiency. It is well known that the structure mass is not determined by the cruise condition but the critical load cases such as gust and manoeuvring loads. Guo et al. [23] highlighted that the gust loads can be larger than the manoeuvring loads, and generate the most critical load cases that some aircraft will experience in flight. Figure 2 demonstrates the spanwise load distributions on a typical civil transport aircraft under cruise and gust encountering conditions, respectively.

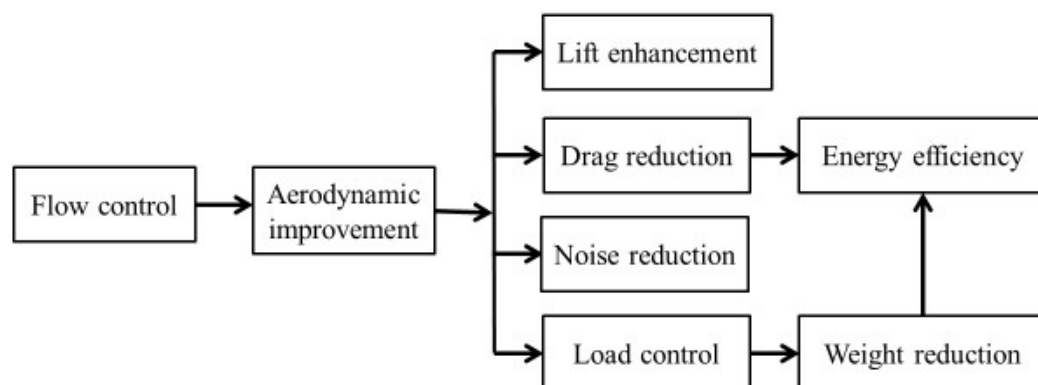


Figure 1. Relationship among flow control, load control and energy efficiency.

Compared to the cruise condition, the spanwise loading especially on the wing experiences a significant increase when the aircraft encounters a gust. This increase will affect the riding comfort of the passengers, and sometimes can be detrimental for the aircraft structure safety if the gust load is severe enough. For the safety of large commercial aircraft, airworthiness authorities have specified typical gust models as a requirement for the certification specifications of large commercial aircraft covered by European Union Aviation Safety Agency Certification Specifications (EASA CS-25) [24].

To cope with these critical load cases, aircraft structures need to withstand the forces and stress caused by gusts with a large amount of mass penalty, since it is challenging to build the structure that is both light and robust. However, if the load can be effectively alleviated through a control means, lighter structures may be used, resulting in the reduction in lift-induced drag and fuel consumption as shown in Figure 1. In the late 1970s, flaps, spoilers and ailerons were investigated to perform the additional task for gust load alleviation. Gust load alleviation (GLA) systems were studied and tested. The first commercial airplane to incorporate a GLA system using ailerons is the Tristar L-1011 from the 1980s [25] after the successful implementation of GLA technology on C-5A [26]. The effectiveness of GLA systems consisting ailerons and spoilers were tested on Airbus A300 [27] and firstly implemented on Airbus A320 [28]. The implementation of a GLA system on the Airbus A300 was shown to mitigate gust load significantly [25]. A baseline wing of a transonic transport aircraft integrated with a GLA system can lead to a reduction in the direct operating cost of nearly 6% and fuel savings of 9% [29]. A 15% wing root bending moment was relieved by the GLA system during unsteady wind encounters on A320 [28].

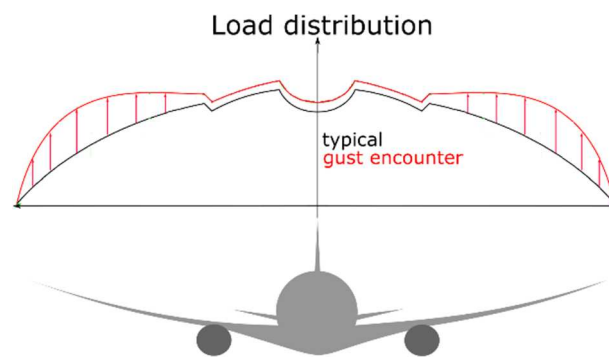


Figure 2. The sketch of the spanwise load distributions under cruise and gust encountering conditions (from [30]).

Currently, for gust load alleviation, active control flaps are deflected to create forces and moments to attenuate gust loads. Ailerons, elevators or spoilers are normally used as the control surfaces for gust load alleviation. Fluidic actuators, such as blowing or suction, synthetic jets and oscillating jets, have been studied for many decades in the field of active aerodynamic flow control. Most of the studies focused on changing the momentum balance in the boundary layer to achieve aerodynamic improvement, such as lift augmentation, drag reduction and stall delay.

Recently, there have been renewed interest in fluidic actuators for their potential application for modern aircraft flight control. Being able to fly and control aircraft without conventional control surfaces (namely flapless control) is one of the targets for future aircraft design with benefits including fewer moving parts, possibly less weight [31], less maintenance and enhanced stealth characteristics [32]. Apart from the steady load control capability, the dynamic responses of these fluidic actuators for unsteady load control, such as gust load, are the key factor for successively replacing the traditional flaps for flight control.

This paper focuses on an overview of the research progress of flow control on gust load alleviation. Gust load definitions and the types of gusts aircraft may be subjected to are introduced. Current gust load alleviation techniques are discussed, followed by a focus on the overview of the studies on gust load alleviation by fluidic actuators including the surface jet blowing and circulation control via Coanda effect. The effects on gust load alleviation through traditional flaps and fluidic actuators are compared and discussed.

2. Basics of Gust Load Alleviation

2.1. Gust Load Definition

Gust, being a complicated phenomenon, is often referred to as atmospheric turbulence. The following two idealized categories of gusts are generally considered in industry for aircraft design, namely [33]: (1) Discrete gusts: the instantaneous gust velocity profile is usually defined by a deterministic form, such as ‘one-minus-cosine’ and ‘sharp-edged’ shapes and (2) Continuous turbulence: the gust velocity varies randomly.

2.1.1. Discrete Gusts

‘One-minus-cosine’ gust is the typical discrete gust defined by the certification specifications of large commercial aircraft covered by the EASA CS-25 [24]. The gust profile is shown in Equation (1) and according to EASA CS-25, the gust shape can be expressed as

$$w_g(x_g) = \frac{w_{g0}}{2} \left(1 - \cos\left(\frac{2\pi x_g}{L_g}\right) \right), \quad 0 \leq x_g \leq L_g \quad (1)$$

where, w_{g0} is the magnitude of the peak gust velocity; L_g is the gust wavelength or twice the ‘gust gradient’ H_g . According to EASA CS-25, the gust wavelength is in the range from 9 to 107 m. In practice, the typical value is $12.5 \bar{c}$ (\bar{c} is the mean aerodynamic chord length).

The design gust velocity w_{g0} changes with gust wavelength and altitude which is expressed in relations of the gust gradient H_g (in m), the reference gust velocity w_{ref} and the flight profile alleviation factor F_g , as

$$w_{g0} = w_{ref} F_g \left(\frac{H_g}{106.17} \right)^{\frac{1}{6}} \quad (2)$$

where, w_{ref} decreases linearly from 17.07 m/s equivalent airspeed (EAS) at sea level to 13.41 m/s EAS at 4572 m and then again to 6.36 m/s EAS at 18,288 m. The flight profile alleviation factor F_g is related to the aircraft weight and the maximum operating altitude [33].

$$F_g = \frac{1}{2} [F_{gz} + F_{gm}] = \frac{1}{2} \left[\left(1 - \frac{Z_{m0}}{76,200} \right) + \sqrt{R_2 \tan \left(\frac{\pi R_1}{4} \right)} \right] \quad (3)$$

$$R_1 = \frac{W_{MLW}}{W_{MTOW}}, \quad R_2 = \frac{W_{MZFW}}{W_{MTOW}} \quad (4)$$

where, Z_{m0} is the maximum operating altitude, W_{MLW} is the maximum landing weight, W_{MZFW} is the maximum zero-fuel weight and W_{MTOW} is the maximum take-off weight.

Assuming an aircraft cruising with the speed U_∞ and encountering a one-minus-cosine gust, the gust penetrating distance is $x_g = U_\infty t$, and Equation (1) can be rewritten as

$$w_g(x_g) = \frac{w_{g0}}{2} \left(1 - \cos \left(\frac{2\pi U_\infty t}{L_g} \right) \right) = \frac{w_{g0}}{2} (1 - \cos(\omega t)) \quad (5)$$

An equivalent gust frequency can be obtained as $\omega = \frac{2\pi U_\infty}{L_g}$ in radians or $\omega = \frac{U_\infty}{L_g}$ in Hz.

2.1.2. Continuous Gusts

Unlike the discrete gusts with a deterministic-form gust velocity profile, the continuous gust velocity varies randomly. The spectrum is normally expressed as a power spectral density as:

$$\Phi(\omega) = \sigma^2 \frac{L_g}{\pi} \frac{1 + \frac{8}{3}(1.339L_g\omega)^2}{\pi [1 + (1.339L_g\omega)^2]^{11/6}} \quad (6)$$

where, the typical wavelength of the continuous gust is defined in EASA CS-25 [24] as 762 m and the frequency is given by ω , rad/m. σ is the root mean square value representing the fluctuations of the gust velocity.

2.2. Gust Load Control Strategies

As mentioned previously, flaps, such as ailerons, elevators or spoilers are normally used as the control surfaces for gust load alleviation. A complete gust load control system includes controllers, actuators and sensors. This control system is commonly called as Gust Load Alleviation (GLA) system. Sensors, such as air data sensors and accelerometers, are located on the aircraft body or wing to sense the incoming wind conditions and to provide feedback of dynamic loads. The general principle of gust load alleviation is to use sensors to provide motion feedback signals for the controllers. The controllers then initiate corresponding deflections of the control surfaces to create the aerodynamic forces and moments needed for attenuating the extra load induced by the gusts. Activating the control surfaces timely can determine the effectiveness of a GLA strategy. Detection of incoming gusts ahead of the aircraft to create a feedforward input is important. This provides control surfaces with additional time to respond. Currently, to compensate the lag of the control surface, it is common to locate the sensors ahead of the wings, along the fuselage, to provide the hydraulic actuators longer time to respond. A high-resolution

direct-measuring short-pulse ultraviolet (UV) Doppler lidar system was designed and tested on an Airbus A340 [34]. It was shown that a forward detection range of 50 m of the atmosphere disturbances was achieved, which translates to a lead time of 300 ms for control surfaces to perform.

Control methods can be categorized as either passive or active. Currently, the widely used gust load control system is active. Passive gust load control devices are more attractive as no extra energies are required compared to the active ones, and initial research has been conducted as being introduced in the following section. Open and closed-loop controls are commonly used by the GLA system. Closed-loop control utilizes feedback to compare the actual output with the desired output. For a successful closed-loop control system, the effective control laws [35,36] play an important role. Various control laws for GLA system have been investigated, such as the linear quadratic regulator theory [37,38], linear quadratic Gaussian method [39,40], and optimal control algorithms [41]. As this article focuses on the overview of the flow control devices for gust load alleviation, the progress in the control laws will not be covered further here.

3. Flow Control Devices for Gust Load Alleviation

Flow control devices for gust load alleviation are categorized into two parts here, i.e., control surfaces or control flaps and fluidic actuators. As being discussed in the following section, traditional control flaps have been revealed to be ineffective for typical high-frequency gust load controls [42,43]. More effective and novel gust load alleviation methods with fast response, such as passive control methods with control surfaces and active control methods using fluidic actuators have been explored and investigated.

3.1. Traditional Control Surfaces

The research on GLA systems was initially motivated by aircraft manufacturers to find ways for structural weight reduction so as to improve fuel efficiency. In 1975, the Lockheed-Georgia Company incorporated a GLA system using wing-outboard ailerons on the C-5A military aircraft. As shown in the flight tests, approximately half of the wing root bending moments was reduced under gust conditions. The dramatic effectiveness and benefits of the GLA system shown on C-5A attracted much attention of the commercial aircraft manufacturers. Later, the GLA system using ailerons was installed on Tristar L-1011 from the 1980s [25], making it the first commercial airplane to incorporate a GLA system. Implementation of a gust load alleviation system incorporating ailerons, spoilers and elevators was then studied for Airbus A300. The effectiveness of different control surfaces was investigated.

3.1.1. Trailing-Edge Flaps

Trailing-edge flaps, known as plain flaps such as ailerons and elevators encompass the aft portion of the wing [44]. The trailing-edge flaps operate by rotating up or down to achieve a desired change in camber, and thus results in a desired change in lift [45]. Lift enhancement is realized by rotating the flap downward, which can be considered as an effective increase in the airfoil camber. When the flap is rotated upwards instead, a negative camber with mitigating lift is realized. On the commercial aircrafts, these trailing-edge flaps play a more important role as the high-lift device. It has been shown that the change in lift achieved by the flaps depends on the chordwise extent of the flap. Unsurprisingly, larger flap sizes have been shown to create larger changes in lift [46]. Therefore, to make a significant lift change, they tend to be relatively large sized and therefore heavy, taking up a large portion of the wing. As a high-lift device, the capability of the steady-state lift augmentation under a constant flap deflection angle is the key. However, as a gust alleviation device, apart from the capability of the lift reduction achieved by the flaps, the characteristics of these flaps under dynamic activations are also vitally important.

On a supercritical airfoil equipped with a spoiler and a flap for a two-dimensional flow, Costes et al. [47] investigated the unsteady aerodynamic performance under subsonic

flow. It was found that for the trailing-edge flap, the lift coefficient decreases significantly with the flap rotating frequency, therefore reducing the range in lift coefficient change to the steady state. Bak et al. [48] also noted that the amplitude of lift change decreases with frequency. Hysteresis loops of the lift changes were present as a function of the flap deflection angle, indicating time lags in the dynamic responses. It was found that for the oscillating the aileron in a sinusoidal pattern, the range of lift coefficient change becomes smaller with angle of attack. For example, at a low angle of attack of $\alpha = 4.6^\circ$, the total lift change is 0.11, while this value is only 0.01 when the angle of attack is 19° , for a fixed reduced frequency of $k = 0.082$.

3.1.2. Spoilers

Spoilers are multifunctional control devices on the upper wing surface, serving a variety of tasks in the flight control system of modern airliners [49]. Spoilers are typically positioned along the upper surface of the wing. Unlike the high-lift devices mentioned above, spoilers are mainly used as an inflight speed brake by rotating to induce a controlled flow separation and thus reducing the lift and increasing the drag. For the inflight speed brake system, the deflection rate of spoilers is rather low, and the dynamic characteristic is not the key factor. However, for an effective GLA system, the deflection rate should be much higher to counteract the high-frequency gusts. Therefore, the dynamic performance of spoilers under unsteady activations requires better understanding. On a 2-D airfoil, Mack et al. [50] found that the incremental lift loss of the spoiler with the increasing deflection angle is quite nonlinear.

Wentz et al. [51] conducted parametric influences of the spoiler geometry on its aerodynamic characteristics. It was found that the vertical distance from the spoiler tip to the trailing edge of the airfoil acted a more important role than that of the chord or deflection angle of the spoiler. For the spoiler location, Maskell [52] found that placing the spoiler at $x/c = 0.4$ failed to reattach flow along the surface, unlike the spoiler at $x/c = 0.2$ for a given deflection angle of $\delta = 40^\circ$ at $\alpha = 4^\circ$. Croom et al. [53] suggested spoilers to be located downstream on swept wings in order to achieve analogous effects like that on unswept wings.

Siddalingappa and Hancock [54] conducted a comprehensive study of 2D and 3D spoilers on the unsteady flow patterns. Transient lag effects were observed during spoiler deployment and the lagging effects increased with the spoiler hinge line locating forward to the airfoil leading edge. Additionally, an initial lift overshoot rather than lift reduction was noticed during their experiments with fast spoiler deployment. This was later called as adverse lift effect by Mabey [55]. During their experiments, it was also found that spoilers on 3D wings had higher effectiveness than that of the 2D aerofoils. It was pointed out that it was due to reduced reattachment length behind the spoiler because of the interaction of vortices from spoiler tip and edges.

The time lag during dynamic spoiler deployment was also observed by Hancock [56], who also revealed a hysteresis effect. Mabey [55] introduced a non-dimensional time to quantify the spoiler deployment rate as $s = \frac{U_\infty t}{c}$, with c being the chord length of the airfoil and U_∞ the incoming flow velocity. It was found that the adverse lift effect is dependent to the non-dimensional time. When the non-dimensional time was less than 5, the adverse lift effect would be observed. However, during the experiments on harmonically oscillating spoilers by Consigny et al. [57], the adverse lift was observed for deployment times up to 9. During the experimental work to investigate the adverse lift by Kalligas [58], no adverse lift was observed for deployment times above 8.

Consigny et al. [59] also found that larger deflection angles did not mean greater changes in lift. It was found that lift remained relatively constant until the spoiler was sufficiently inclined to prevent separated flow downstream of the spoiler from reattaching. However, the low spoiler angle ($\delta = 1^\circ$) was shown to be ineffective at separating the flow. This is due to the height of the spoiler being too small, which is mentioned previously that the extent of the separated region being proportional to the spoiler height. The finding was

opposite by Costes et al. [47], as lower deflection angles produce greater force variation than larger deflection angles. Meanwhile, this statement was given under the result of the unsteady force variation with $\delta = 5^\circ$ which was greater than twice the amplitude observed at $\delta = 10^\circ$. From these findings, it can be seen that the deflection angle should be high enough to make sure a certain degree of spoiler height.

Harmonic oscillations of spoilers were also investigated by Nelson et al. [59]. During their studies, it was found that the nonlinearities of a rapidly deploying spoiler increased with reduced frequency (oscillating rate). The reduced frequency also has influence on the spoiler effectiveness. It was found by Consigny et al. [57] that the amplitude in change in lift coefficient became smaller with larger reduced frequencies, accompanied by greater phase delays. Mineck [60] extended the investigations of spoilers to transonic conditions with a consideration of Reynolds effects up to a flight Reynolds number of 30 million. It was found that the effectiveness of the spoiler increased with the Reynolds numbers increasing from 3 million up to 22 million. Meanwhile, a further Reynolds number increase up to 30 million saw almost no changes. To provide validation data of manoeuvring flaps for CFD methods, the German Aerospace Center (DLR) developed a wind tunnel model with an active spoiler [49,61] to investigate the aerodynamic characteristics of static and dynamic spoiler deflections.

3.2. Non-Traditional Control Surfaces

As mentioned previously, traditional control surfaces commonly take up a large portion of the wing section and thus tend to be heavy with slow responses. This prevents the control surfaces from high-frequency activations. Therefore, the effectiveness of the traditional control surfaces for high-frequency gust load alleviation is rather limited. As these control surfaces have other tasks for flight control, such as high-lift devices or inflight speed brakes, the size of these control surfaces should be balanced for their functions. Non-traditional control surfaces are relative to the above-mentioned flaps. These control surfaces use newer technology and 'smart' materials for fast activation. These control surfaces have been investigated mainly for wind turbines for gust load alleviation, such as the compact trailing-edge flap [62], the adaptive compliant wing [63], the adaptive trailing-edge geometry [48,64] and the microtabs [65,66]. Comprehensive overviews of these active flow control methods for wind turbines are presented by Johnson et al. [67,68].

3.3. Passive Control Devices

Comparing with the active control system, a passive control device is usually simpler and does not rely on extra energy. Guo et al. investigated the effects of a passive twist wingtip as a gust-load alleviation device on a flying-wing configuration [69] and a 200-seater airliner [23], respectively. This concept is to use a separate wing-tip section connected to the main wing by a spring. As the shaft is located ahead of the aerodynamic centre, this device will have a nose-down twist under the gust-induced aerodynamic force resulting in gust load alleviation. The results showed significant reduction in gust-induced wing-tip displacement and root bending moment. Compared to the current active control methods, this passive control concept is attractive as it requires no energy input.

Similar to the ideas by Guo et al., Castrichini et al. [70–72] investigated the effects for the alleviation on wing root bending moments at gust conditions by a flexible wing-fold device. The key idea was to introduce a hinge line which was not parallel to the incoming flow direction but was rotated outboard with a hinge orientation Λ to allow the wing tip to rotate. Therefore, folding the wingtip with the angle of θ will reduce the local angle of attack, which can be calculated as $\Delta\alpha = -\tan^{-1}(\tan\theta\sin\Lambda)$. The results indicated that suitable designs of the control device are capable for gust load alleviation. It was also observed that the load alleviation capabilities are highly sensitive to the stiffness of the hinge spring and the wing-tip mass. It will be a problem in application as it is very challenging practically to change the mass or the hinge spring stiffness according to different incoming flows.

3.4. Fluidic Actuators

As a means for active aerodynamic flow control, fluidic actuators, including synthetic jets, circulation control using Coanda effects, jet blowing and suction, have been investigated extensively. These methods have been shown to be effective for aerodynamic improvements through boundary-layer modulation, such as drag reduction [73,74], delay of transition [75,76] and flow separation control [10,77,78], flow improvement for air intakes [79,80], stall control and lift augmentation [81,82].

Flow control for load control is currently attractive for modern aircraft design, as it has the potential for flapless control with benefits including fewer moving parts, possibly less weight [31], less maintenance and enhanced stealth characteristics [32]. A few studies have been carried out to evaluate the capability of fluidic actuators known as jet flaps. The jet flap consists of a narrow slot extending across the wing surface, which ejects high momentum air [83]. For blowing tangentially near the trailing edge on an airfoil surface, the airflow will closely follow the profile of the surface due to the Coanda effect. The control method making use of the Coanda effect at the trailing edge can directly manipulate the airfoil circulation and is therefore called Circulation Control (CC).

3.4.1. Surface Jet Blowing

For normal surface jet blowing, the jet flow disrupts the main flow, leading to flow separation [84]. A separation bubble emerges to encompass the surface up to the trailing edge. An alteration in the Kutta condition is then realised as the separation bubble encourages flow to be entrained from the freestream flow around the wing surface, thereby modulating the circulation created by the wing [85]. Consequently, the load on the wing is modified.

Jet actuators have been investigated experimentally for load control on NACA0015 aerofoil for reshaping aeroelastic responses including limit cycle oscillation and flutter by Rao et al. [86]. The results showed an improvement of more than 15% of the flutter speed by the jet actuators using a PID controlled loop [87]. Microjets being small pneumatic jets using high-speed flow blowing normal to the aerofoil or wing surface have been studied as approaches for load control.

de Vries et al. [88] conducted numerical studies of a non-rotating NACA0018 aerofoil with microjets located near the trailing edge under freestream Mach number of 0.176. Significant changes in lift were observed for the angle of attack ranging from -10° to 10° . Moreover, the results also showed that approximately 50% of the total change in the lift could be obtained within the non-dimensional time $s = \frac{U_\infty \Delta t}{c} = 1$, indicating its rapid load control response characteristic. Blaylock et al. [66,85] compared the load control effects of microjets and microtabs deployed on the NACA0012 aerofoil trailing edge. The results showed that both concepts had a similar load control mechanism by affecting the trailing-edge flow, and therefore produced very similar aerodynamic load control effects.

Heathcote et al. [89] conducted wind tunnel tests for comparing the effects of blowing (microjets) and microtabs, and pointed out that blowing and microtabs were viable methods for load control but with very different behaviours: the blowing deflected the wake upwards thereby reducing lift, conversely the microtabs promoted separation over the upper surface resulting in lift reduction. They also noted the nearly constant lift change across all angles of attack by microjet blowing located at the trailing edge, which was constant with the result drawn by de Vries et al. [88].

However, for microtabs, optimal location varied according to the angle of attack. At small ones, it is preferable to place the microtabs near the trailing edge, while locations near the leading edge were better when the angle of attack is high. de Vries et al. [88] performed numerical studies at the steady condition on the NACA0018 aerofoil at $M_\infty = 0.176$ with a normal jet placed on the upper surface trailing edge and a significant lift reduction was obtained. Al-Battal et al. [43] assessed the capability of blowing for lift reduction experimentally. Two different blowing directions, normal and upstream, from the upper surface of the NACA0012 aerofoil under the steady incoming flow velocity of 20 m/s and a range of angles of attack from 0° to 20° were compared. The results indicated

that the chordwise location of normal blowing had a dramatic influence on the load control effectiveness in terms of lift reduction. Normal blowing at $x/c = 0.95$ induced a lift coefficient decrease of 0.15 under the maximum blowing momentum coefficient (momentum coefficient is defined as $C_\mu = \frac{\dot{m}U_{jet}}{q_\infty A}$, where, \dot{m} is the mass flow rate through the jet slot exit, q_∞ is the dynamic pressure of the freestream, A is the surface area of the wing and U_{jet} is the jet velocity). However, moving the microjet further forward, the lift change was negligible and even no lift decrease was induced when normal blowing was placed near the leading edge.

For the influence of jet-slot location and jet-slot width on the lift reduction effects by normal blowing, the authors conducted numerical studies based on the NACA0012 airfoil [30]. Figure 3 gives the results of lift coefficient reduction ($\Delta C_L = C_{L, with\ jet} - C_{L, without\ jet}$) against the jet-slot locations under $M_{jet} = M_\infty = 0.3$ at $\alpha = 0^\circ$ and 3° . It is clear that the magnitudes of the reduction in lift coefficient increase with microjets moving towards the trailing edge, and this trend is captured both at $\alpha = 0^\circ$ and 3° . The trend of positioning the jet towards the trailing edge enhancing lift is consistent to the findings by Lockwood and Vogler et al. [90], Mikolowsky and McMahon [91]. At $\alpha = 0^\circ$, the reduction in lift coefficient of $\Delta C_L = -0.09$ is obtained due to the microjet blowing at $x/c = 0.4$, and this value reaches to $\Delta C_L = -0.33$ when the microjet moves to $x/c = 0.95$. Noticeably, the magnitudes of lift coefficient reduction increase almost linearly with the microjet location moving from $x/c = 0.7$ to 0.95 for both $\alpha = 0^\circ$ and 3° . For the influence of jet-slot width, it is shown that the magnitude of lift reduction increases with the increase in jet slot width. It is more obvious when the jet slot width is below $0.5\%c$, as the value of lift reduction tends to be stable when the slot width increases from $0.5\%c$ to $1.0\%c$. Meanwhile, it is undeniable that a smaller width of the jet exit will be preferable since it is undeniable that the slots will bring discontinuity to the wing surfaces [92]. Figure 4 presents the comparisons of the surface pressure coefficients between the baseline model and the models with microjet blowing. Figure 5 displays the velocity flow fields of the models with microjets located at $x/c = 0.4$ and $x/c = 0.9$ at $\alpha = 0^\circ$.

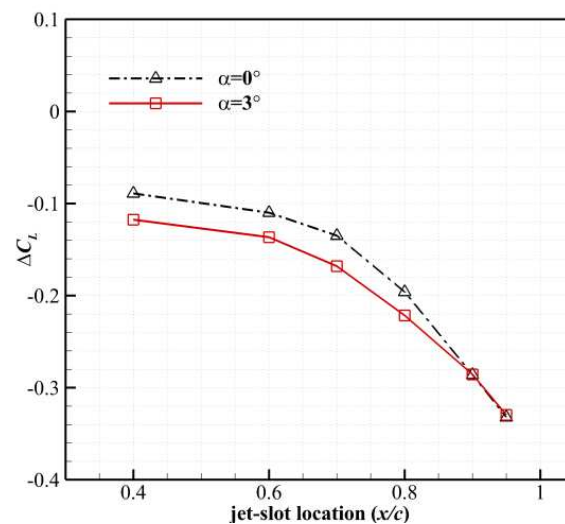


Figure 3. Influence of Microjet location on lift coefficient reduction with $M_{jet} = M_\infty = 0.3$ (from [30]).

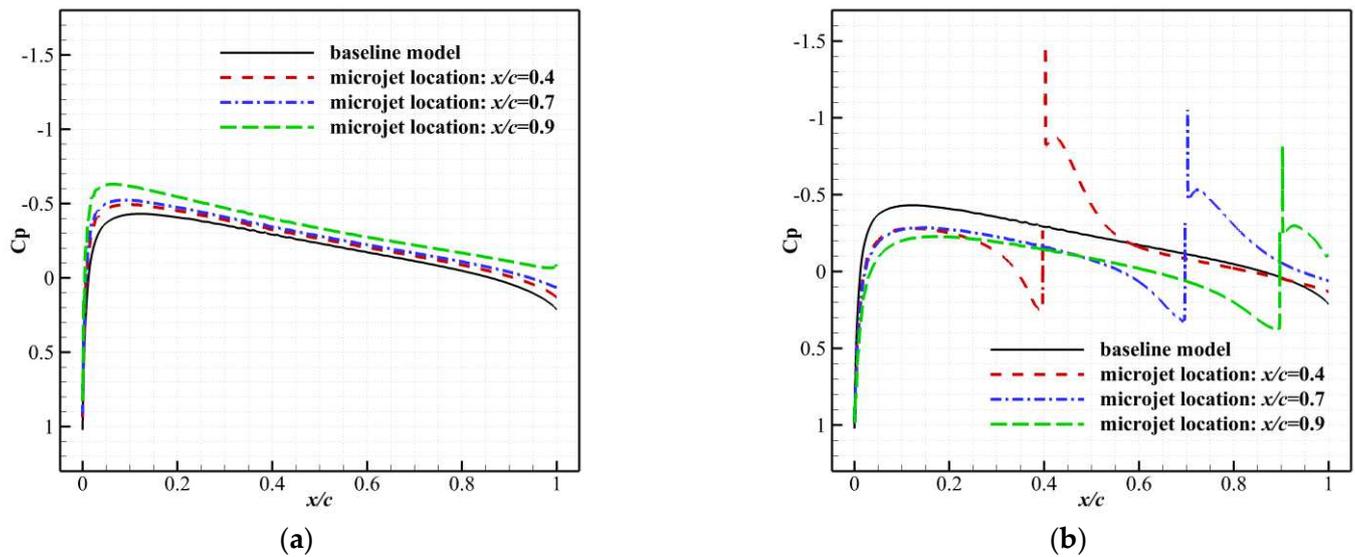


Figure 4. Comparisons of pressure coefficients between the baseline model and microjet blowing models at $M_\infty = 0.3$, $\alpha = 0^\circ$ (from [30]). (a) Lower surface; (b) Upper surface.

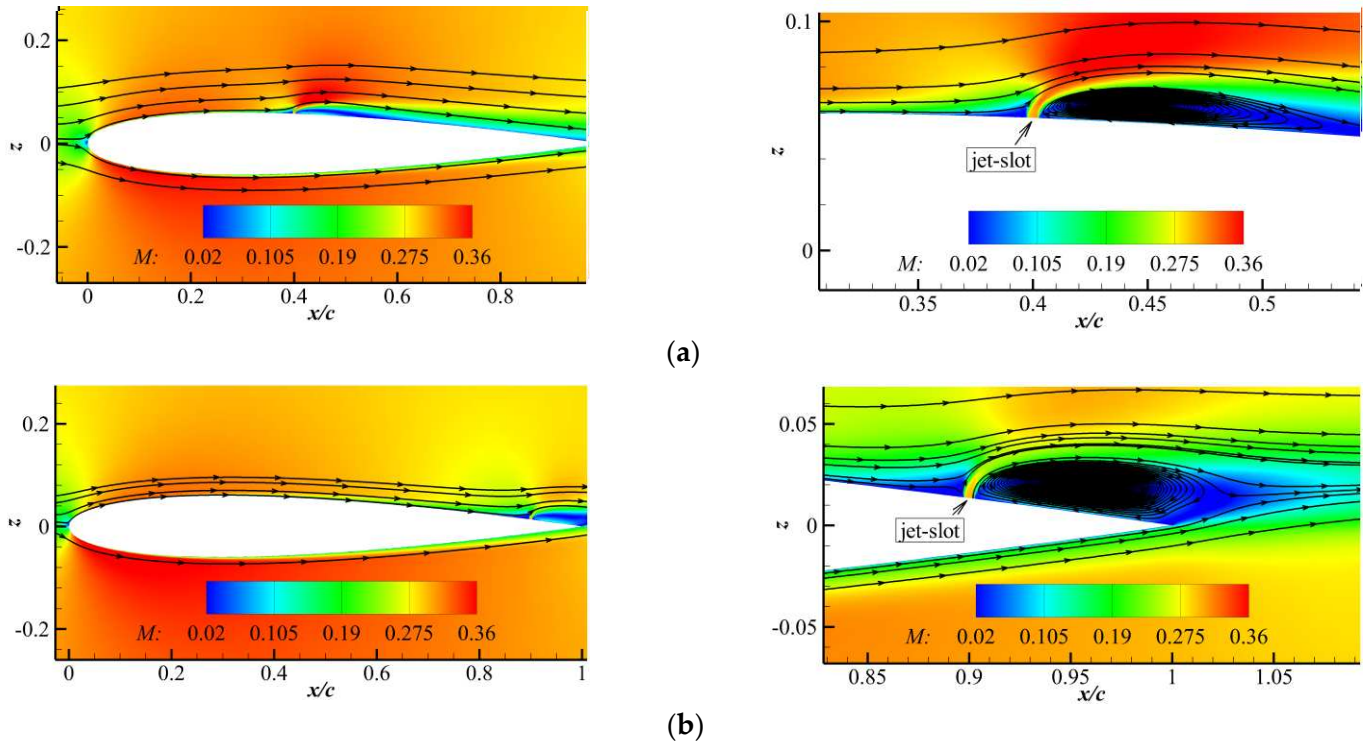


Figure 5. Velocity flow fields and streamlines of the baseline model and models with microjet blowing for $M_{jet} = M_\infty = 0.3$, at $\alpha = 0^\circ$ (from [30]). (a) Microjet blowing, $x/c = 0.4$; (b) microjet blowing, $x/c = 0.9$.

Also shown is the region of interest around the microjets and the trailing edges. From these results, it can be concluded that blowing generates a separation region near the jet location, and the separation region is more apparent after the jet location than that before it. This separation region deflects the streamlines upwards near the jet location and blocks the flow over the upper surface. This increases the upper surface pressure coefficients ahead the blowing slot. However, behind the jet slot, the pressure recovers rapidly. From Figure 5, it can be seen that this separation not only deflects the streamline above the upper surface, but also entrains the flow from the lower surface upwards. This entrainment accelerates the flow under the lower surface and results in a reduction in the pressure coefficients on the

lower surface. Also shown is that the entrainment capability is stronger when the blowing is placed towards the trailing edge, as slight decreases in pressure coefficients are noticed with blowing slot moving towards the trailing edge as demonstrated in Figure 4b. The combined effects explain the reduction in lift coefficient with the normal microjet blowing relative to the baseline model. In [92], the authors also demonstrated that normal microjet blowing has a stronger capability for load control at transonic incoming flow as normal microjet blowing show strong influence on the shock strength on the airfoil upper surface. For a 3D wing with jet slot only deployed near the wing tip, the effects of blowing have an extension to the whole wingspan.

For the properties of blowing under unsteady actuations, a further experiment of the upstream blowing was conducted by Al-Battal et al. [93]. The time lag in lift responses corresponding to blowing actuation frequency has been observed due to the change in the circulation and the vorticity shedding. The time delay became more significant with increasing angles of attack because of more separated flow. The effects of the slot blowing on unsteady aerodynamic load control with a freestream velocity from 6.7 m/s to 22.2 m/s on NACA0018 airfoil was experimentally evaluated by Mueller-Vahl et al. [94]. The results showed that the lift oscillation due to the unsteady incoming flow can be effectively counteracted by dynamically adapting the slot blowing velocity. For the further understanding of the behaviour of the dynamic actuations, the responses of microjet blowing with periodic actuations are evaluated at by the authors in [92]. It was demonstrated that the microjet blowing is also effective under dynamic actuations. However, the load control effect is reduced with the increase in blowing frequency.

Based on the load control capabilities of microjet blowing under steady and unsteady actuations, its capabilities for gust load alleviation was evaluated by the authors in Ref. [92] on the 2-D NACA0012 and 3-D BAH wing. The test cases show that normal microjet blowing is a promising approach for gust load alleviation with a fast frequency response characteristic. The results of gust load alleviation on both the 2-D airfoil and the 3-D BAH wing verify that microjet blowing is able to suppress the gust load disturbances. Due to the fast response characteristics, it is capable for timely adaptive gust load control. For the test cases of rigid BAH wing, a significant reduction in gust-induced lift and root bending moment coefficients has been achieved. Because of the alleviation in gust load, significant suppression of the gust-induced disturbances in the displacement and acceleration has been obtained in the case study on the elastic BAH wing. Due to the fast-response characteristics of microjet blowing, a near constant lift response under gust condition is obtained by adaptively adjusting the blowing momentum coefficients. Another gust load alleviation study using synthetic jets on the NACA0012 airfoil was conducted by De Breuker, et al. [95]. It was demonstrated that synthetic jets also have the potential for gust load control.

3.4.2. Circulation Control by Jet Blowing through the Trailing-Edge Coanda Device

Circulation Control (CC) using Coanda effect uses tangential surface jets to change the aerodynamic properties of the airfoil or wing. The Coanda effect describes the tendency of a high-speed jet flow staying attached to a convex surface due to the balance between centrifugal forces and low static pressures created by the high-speed jet [96]. The high-speed jet flow entrains the external flow to follow it as to 'bend down' over the curved surface which generates the circulation increase, and thus results in lift augmentation. Similarly, lift reduction can be obtained through placing the jet slots on the lower surface. Conventionally, a CC device system consists of an air plenum, a rounded trailing edge and an orifice which is the slot exit of the CC jet.

The initial intention for the development of the CC system was for short landing and take-off capability, especially by the US Navy, looking for ways to improve aircraft operation from carriers [97]. Many tests including a full-scale flight test and design works have been carried out on the A-6 Intruder [98]. The effectiveness and efficiency of CC for manoeuvrability control of fixed and rotary-wing aircraft have also been researched

through various experiments and numerical studies. After the wind tunnel test on a diamond wing tailless aircraft, Cook et al. [99] pointed out that the CC device exhibited good aerodynamic performance similar to a traditional flap with an equivalent size on a fixed wing under modest blowing momentum coefficients, and the response characteristic was essentially linear.

Experimental and computational work seeking for a design using trailing-edge blowing to eliminate the trailing-edge flaps, or use leading-edge blowing to eliminate the need for leading-edge slats have been carried out on a Boeing 737 aircraft [97,100]. A joint project [32,101,102] has been carried out by University of Manchester, Cranfield University and BAE Systems to demonstrate new technologies for flapless control, and a drone has been designed named MAGMA which finished its first flight trial in 2017. Instead of traditional control surfaces, this project assessed the manoeuvrability of two novel technologies. One is to deploy CC on the wing sections and another one is to use the fluidic thrust vectoring (FTV) placed on the centre body. Engine bleed air is used for the pneumatic supply of the CC and fluidic thrust vectoring effectors. It is shown that the critical flight conditions are climb turns and descending flight where geometric and effort/power saturation limits are met, respectively [103].

To investigate the capability of CC for rolling control on the flying-wing configuration, Hoholis [104] extended a numerical study of CC as a roll effector on the generic SACCON UCAV configuration. This work was performed with a freestream Mach number 0.145 and was concluded that CC can produce similar rolling moments to flaps at low angles of attack. The effects for providing manoeuvrability by CC on a tailless vehicle was evaluated by Wilde et al. [105]. The results show that CC units could provide similar three-axis control effects relative to the split flap elevons.

To explore novel method for gust load alleviation to keep pace with the fast development in control system designs using CC. The feasibility and effects of gust load alleviation by means of CC is firstly numerically studied by Li and Qin [106]. The NACA0012 airfoil was chosen for the study from subsonic to transonic speeds. In this study, CC via steady blowing with different momentum coefficients are firstly tested for the gust load alleviation effects in terms of lift coefficients under a ‘one-minus-cosine’ gust. The results demonstrated that CC can effectively suppress the maximum gust-induced lift increment, but is not feasible for suppressing the unsteady gust-induced lift perturbations. Based on the verified fast-frequency response characteristics of CC, unsteady blowing with dynamically adaptive momentum coefficients proportional to the vertical gust velocities is proposed and tested. The results as shown in Figure 6 demonstrate that a near constant lift coefficient can be achieved under gust condition for subsonic incoming flow indicating its potential for real-time adaptive load control. This study also demonstrated that CC is able to reduce gust load at transonic speed, but it is less effective as compared with that at subsonic speed.

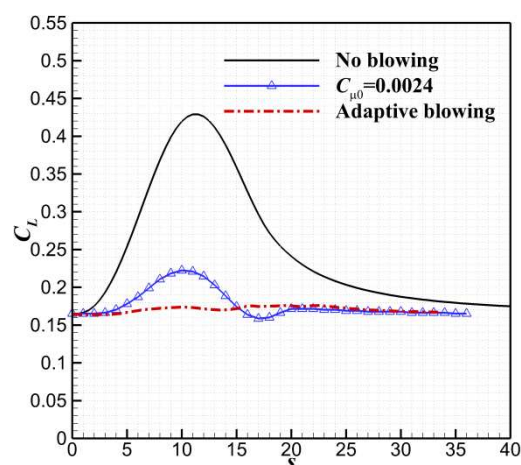


Figure 6. The gust response with and without Circulation Control (from [106]).

The study on the feasibility of gust load alleviation using CC is then extended to a three-dimensional wing including aerodynamic and structure interaction by Li and Qin [107]. Coanda device is deployed on the wing tip (from $\eta = y/l = 0.74$ to 0.98). The spanwise load control effects are firstly evaluated under steady CC jet blowing at different incoming flows as shown in Figure 7. Significant load control effect has been noticed around CC deployment region. Also shown is that apart from this region, CC also has influence on the span load towards the wing root, but with a reducing load control effect. Then, load control effects under dynamic CC jet blowing and gust load alleviation under typical ‘one-minus-cosine’ gust profiles from certification specification defined by European Aviation Safety Agency are tested. The results show a promising capability of CC for gust load alleviation as significant gust load alleviation effects have been achieved for both the rigid and elastic wings. For the wing considering aeroelasticity, the displacement oscillations induced by gusts have been effectively suppressed by CC.

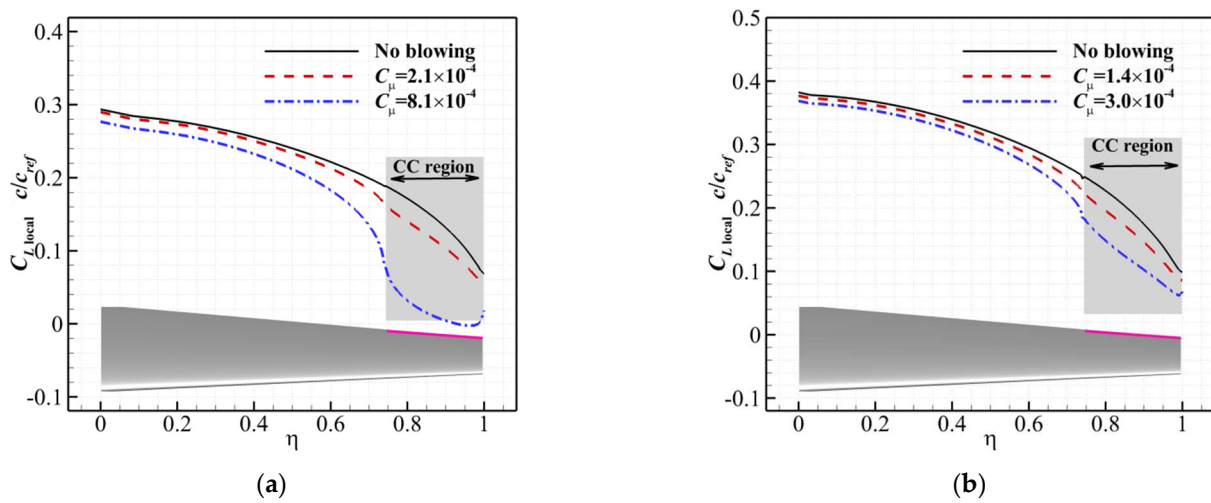


Figure 7. The influence of spanwise load distributions due to CC jet blowing. (a) $M_\infty = 0.3$; (b) $M_\infty = 0.7$.

3.5. Summary of the Characteristics of These Flow Control Devices

Table 1 gives a summary of the advantages and limitations of the flow control devices presented above. Although the traditional control surfaces have been applied to aircraft for gust load alleviations, these devices do not meet the requirements of fuel efficiency for future aircraft design due to their large size and structure weight. Although passive control technologies have been tested in the laboratories, it is still a challenge to improve the robustness and reliability. Active flow control using fluidic actuators show high efficiency and have great application potential for gust load alleviation. However, as it is still a novel technology, there is a lack of comprehensive understanding of flow control mechanism and in-depth research on their applications in the actual flight environment of aircraft.

Table 1. Comparisons of the characteristics of the flow control devices for gust load alleviation.

Flow Control Category	Typical Devices	Advantages	Limitations
Active flow control	Traditional control surfaces: Trailing-edge flaps and Spoilers	Robustness for a large range of incoming flow speeds	large size and heavy low-frequency responses
	Fluidic actuators: Surface jets and CC	high-frequency responses small size and less weight	decreases in gust load alleviation effects with increasing incoming flow speeds
Passive flow control	wingtip twist and flexible wing-fold devices	no extra energy required simple structural mechanism	Poor robustness away from design point

4. Concluding Remarks

In the context of growing concern for environmental protection and reduction in fuel consumption, flow control for gust load alleviation can play a vital role for future greener aircraft design. Some main conclusions can be drawn from the review.

Currently aircraft flow control for gust load control are achieved by deflecting control flaps, such as spoilers or trailing-edge flaps to create forces and moments that needed to alleviate the gust load. Being unsteady aerodynamic disturbances, gusts can have very high frequencies. For an effective gust load alleviation system, the capability of fast responses is the key factor. However, as the traditional flaps acting mainly for high-lift devices and flight manoeuvring, they are normally large sized and therefore heavy. These traditional flaps tend to exhibit low-frequency responses, which are ineffective for high-frequency gusts due to their large inertia.

In order to achieve faster responses, efforts towards smaller flap sizes have been made. However, these efforts have focused only on wind turbines up to now. To make a simpler system compared to the active flow control means which usually require complex actuating systems, passive wing-tip devices have also been studied for gust load alleviation. Passive control means can be designed to be reliable and effective at some flight conditions. It is hard to make them reliable and effective for a wide range of gust conditions.

The flow control methodologies using fluidic actuators are shown to have good potential for load control and flight control to replace the traditional flaps. This results in fewer moving parts, possibly less weight, less maintenance, high-frequency actuations and thus improved aerodynamic performance. This article has introduced two of the most promising actuators, i.e., surface jet blowing and circulation control. It has been demonstrated that both CC and surface jet blowing have a fast response characteristic and the capability for adaptive gust load controls. These actuators still face many engineering challenges. For CC, the main issue is the sharp decrease in load control capability with the increase in freestream velocities. For surface jet blowing including normal blowing and upstream blowing, the load control capability in terms of lift modulation is not as effective as CC at low speeds. Therefore, for industrial applications, more efforts are needed with in-depth investigations on these actuators.

Author Contributions: Conceptualization, N.Q. and Y.L.; Investigation, Y.L.; resources, N.Q.; writing—original draft preparation, Y.L.; writing—review and editing, N.Q. All authors have read and agreed to the published version of the manuscript.

Funding: This research received no external funding.

Institutional Review Board Statement: Not applicable.

Informed Consent Statement: Not applicable.

Data Availability Statement: Not applicable.

Conflicts of Interest: The authors declare no conflict of interest.

Nomenclature

s	non-dimensional time
C_L	lift coefficient
M_{jet}	the Mach number of the jet
C_μ	momentum coefficient
$C_{\mu 0}$	peak value of the momentum coefficient with the one-minus-cosine profile
M_∞	Mach number of the freestream flow
α	angle of attack
U_∞	freestream velocity
C_p	pressure coefficient
c	chord length
c_{ref}	mean aerodynamic chord length
x, y, z	Cartesian coordinates in streamwise, spanwise and vertical directions

References

1. Psarftis, H. *Green Transportation Logistics: The Quest for Win-Win Solutions*; International Series in Operations Research & Management Science; Springer: Berlin/Heidelberg, Germany, 2015; Volume 226.
2. Salam, I.R.; Bil, C. Multi-disciplinary analysis and optimisation methodology for conceptual design of a box-wing aircraft. *Aeronaut. J.* **2016**, *120*, 1315–1333. [[CrossRef](#)]
3. Chakraborty, I.; Nam, T.; Gross, J.R.; Mavris, D.N.; Schetz, J.A.; Kapania, R.K. Comparative Assessment of Strut-Braced and Truss-Braced Wing Configurations Using Multidisciplinary Design Optimization. *J. Aircr.* **2015**, *52*, 2009–2020. [[CrossRef](#)]
4. Colliss, S.P.; Babinsky, H.; Nöbler, K.; Lutz, T. Vortical structures on three-dimensional shock control bumps. *J. Aircr.* **2016**, *53*, 2338–2350. [[CrossRef](#)]
5. Bruce, P.J.K.; Babinsky, H. Experimental Study into the Flow Physics of Three-Dimensional Shock Control Bumps. *J. Aircr.* **2012**, *49*, 1222–1233. [[CrossRef](#)]
6. König, B.; Pätzold, M.; Lutz, T.; Krämer, E.; Rosemann, H.; Richter, K.; Uhlemann, H. Numerical and Experimental Validation of Three-Dimensional Shock Control Bumps. *J. Aircr.* **2009**, *46*, 675–682. [[CrossRef](#)]
7. Ogawa, H.; Babinsky, H.; Pätzold, M.; Lutz, T. Shock-Wave/Boundary-Layer Interaction Control Using Three-Dimensional Bumps for Transonic Wings. *AIAA J.* **2008**, *46*, 1442–1452. [[CrossRef](#)]
8. Messing, R.; Kloker, M.J. Investigation of suction for laminar flow control of three-dimensional boundary layers. *J. Fluid Mech.* **2010**, *658*, 117–147. [[CrossRef](#)]
9. Chernoray, V.G.; Dovgal, A.V.; Kozlov, V.V.; Lfdahl, L. Experiments on secondary instability of streamwise vortices in a swept-wing boundary layer. *J. Fluid Mech.* **2005**, *534*, 295–325. [[CrossRef](#)]
10. Krishnan, K.S.G.; Bertram, O.; Seibel, O. Review of hybrid laminar flow control systems. *Prog. Aerosp. Sci.* **2017**, *93*, 24–52. [[CrossRef](#)]
11. Brion, V.; Dandois, J.; Jacquin, L. Laminar buffet and flow control. In Proceedings of the 7th European Conference for Aeronautics and Space Sciences, Milano, Italy, 3–6 July 2017.
12. Ashill, P.R.; Fulker, J.L.; Hackett, K.C. A review of recent developments in flow control. *Aeronaut. J.* **2005**, *109*, 205–232. [[CrossRef](#)]
13. Joslin, R.D. *Overview of Laminar Flow Control*; NASA/TP-1998-208705; NASA Langley Research Center: Hampton, Virginia, USA, 1998.
14. *Hybrid Laminar Flow Control Study Final Technical Report*; NASA-CR-165930; NASA Langley Research Center: Hampton, VA, USA, 1982.
15. Murai, Y. Frictional drag reduction by bubble injection. *Exp. Fluids* **2014**, *55*, 1773. [[CrossRef](#)]
16. Fuaad, P.A.; Baig, M.F.; Khan, B.A. Turbulent drag reduction using active control of buoyancy forces. *Int. J. Heat Fluid Flow* **2016**, *61*, 585–598. [[CrossRef](#)]
17. Ahmad, H.; Baig, M.F.; Fuaad, P.A. Numerical investigation of turbulent-drag reduction induced by active control of streamwise travelling waves of wall-normal velocity. *Eur. J. Mech. B Fluids* **2015**, *49*, 250–263. [[CrossRef](#)]
18. Wang, Y.-S.; Huang, W.-X.; Xu, C.-X. Active control for drag reduction in turbulent channel flow: The opposition control schemes revisited. *Fluid Dyn. Res.* **2016**, *48*, 055501. [[CrossRef](#)]
19. Liebeck, R.H. Design of the Blended Wing Body Subsonic Transport. *J. Aircr.* **2004**, *41*, 10–25. [[CrossRef](#)]
20. Graham, W.R.; Hall, C.A.; Vera Morales, M. The potential of future aircraft technology for noise and pollutant emissions reduction. *Transp. Policy* **2014**, *34*, 36–51. [[CrossRef](#)]
21. Lebofsky, S.; Ting, E.; Nguyen, N.; Trinh, K. Optimization for Load Alleviation of Truss-Braced Wing Aircraft with Variable Camber Continuous Trailing Edge Flap. In Proceedings of the 33rd AIAA Applied Aerodynamics Conference, Dallas, TX, USA, 22–26 June 2015.
22. Jemitola, P.O.; Fielding, J.P. Box wing aircraft conceptual design. In Proceedings of the 28th International Congress of the Aeronautical Sciences, Brisbane, Australia, 23–28 September 2012.
23. Guo, S.; Los, J.; Liu, Y. Gust Alleviation of a Large Aircraft with a Passive Twist Wingtip. *Aerospace* **2015**, *2*, 135–154. [[CrossRef](#)]
24. European Aviation Safety Agency. *Certification Specifications for Large Aeroplanes CS-25*; European Aviation Safety Agency: Cologne, Germany, 2008.
25. Johnston, J.F. *Accelerated Development and Flight Evaluation of Active Controls Concepts for Subsonic Transport Aircraft. Volume 1: Load Alleviation/Extended Span Development and Flight Tests*; NASA-CR-159097; NASA Langley Research Center: Hampton, VA, USA, 1979.
26. Disney, T.E. C-5A Active Load Alleviation System. *J. Spacecr. Rocket.* **1977**, *14*, 81–86. [[CrossRef](#)]
27. Al-Battal, N. Flow Control for Loads Control. Ph.D. Thesis, University of Bath, Bath, UK, 2019.
28. Payne, B.W. Designing a Load Alleviation System for a Modern Civil Aircraft. In Proceedings of the 15th Congress of the International Council of the Aeronautical Sciences, London, UK, 7–12 September 1986. ICAS-86-5.2.3.
29. Xu, J.; Kroo, I. Aircraft Design with Maneuver and Gust Load Alleviation. In Proceedings of the 29th AIAA Applied Aerodynamics Conference, Honolulu, Hawaii, 27 June 2011. AIAA Paper 2011-3180.
30. Yonghong, L. Gust Load Alleviation by Fluidic Actuators on a Blended-Wing-Body Configuration. Ph.D. Thesis, Sheffield University, Sheffield, UK, 2020.
31. Paterson, E.; Baker, W.; Kunz, R.; Peltier, L. RANS and Detached-Eddy Simulation of the NCCR Airfoil. In Proceedings of the 2004 Users Group Conference (DOD_UCG'04), Williamsburg, VA, USA, 7–11 June 2004; pp. 112–122.

32. Anonymous. BAE Systems success in flapless flight. *Aircr. Eng. Aerosp. Technol.* **2006**, *78*. [[CrossRef](#)]
33. Wright, J.R. *Introduction to Aircraft Aeroelasticity and Dynamic Loads*, 2nd ed.; Cooper, J.E., Ed.; Wiley: Chichester, UK, 2015.
34. Rabadan, G.J.; Schmitt, N.P.; Pistner, T.; Rehm, W. Airborne Lidar for Automatic Feedforward Control of Turbulent In-Flight Phenomena. *J. Aircr.* **2010**, *47*, 392–403. [[CrossRef](#)]
35. Alam, M.; Hromcik, M.; Hanis, T. Active gust load alleviation system for flexible aircraft: Mixed feedforward/feedback approach. *Aerosp. Sci. Technol.* **2015**, *41*, 122–133. [[CrossRef](#)]
36. Liu, J.; Zhang, W.; Liu, X.; He, Q.; Qin, Y. Gust response stabilization for rigid aircraft with multi-control-effectors based on a novel integrated control scheme. *Aerosp. Sci. Technol.* **2018**, *79*, 625–635. [[CrossRef](#)]
37. Fazelzadeh, S.A.; Jafari, S.M. Active control law design for flutter suppression and gust alleviation of a panel with piezoelectric actuators. *Smart Mater. Struct.* **2008**, *17*, 035013. [[CrossRef](#)]
38. Patil, M.J.; Hodges, D.H. Output Feedback Control of the Nonlinear Aeroelastic Response of a Slender Wing. *J. Guid. Control Dyn.* **2002**, *25*, 302–308. [[CrossRef](#)]
39. Liu, X.; Sun, Q.; Cooper, J.E. LQG based model predictive control for gust load alleviation. *Aerosp. Sci. Technol.* **2017**, *71*, 499–509. [[CrossRef](#)]
40. Liu, X.; Sun, Q. Improved LQG Method for Active Gust Load Alleviation. *J. Aerosp. Eng.* **2017**, *30*, 04017006. [[CrossRef](#)]
41. Frost, S.; Taylor, B.; Bodson, M. Investigation of Optimal Control Allocation for Gust Load Alleviation in Flight Control. In Proceedings of the AIAA Atmospheric Flight Mechanics Conference, Minneapolis, MN, USA, 13–16 August 2012. AIAA 2012-4858.
42. Al-Battal, N.; Cleaver, D.; Gursul, I. Lift reduction by counter flowing wall jets. *Aerosp. Sci. Technol.* **2018**, *78*, 682–695. [[CrossRef](#)]
43. Al-Battal, N.; Cleaver, D.; Gursul, I. Aerodynamic Load Control through Blowing. In Proceedings of the 54th AIAA Aerospace Sciences Meeting, San Diego, CA, USA, 4–8 January 2016. AIAA 2016-1820.
44. Abbott, I.H.; Doenhoff, A.E. *Theory of Wing Sections: Including a Summary of Airfoil Data*; Dover Publications, Inc.: New York, NY, USA, 1959.
45. Anderson, J.D. *Introduction to Flight*, 8th ed.; McGraw-Hill Education: New York, NY, USA, 2016.
46. Frederick, M.; Kerrigan, E.C.; Graham, J.M.R. Gust alleviation using rapidly deployed trailing-edge flaps. *J. Wind Eng. Ind. Aerodyn.* **2010**, *98*, 712–723. [[CrossRef](#)]
47. Costes, M.; Gravelle, A.; Philippe, J.; Vogel, S.; Triebstein, H. Investigation of Unsteady Subsonic Spoiler and Flap Aerodynamics. *J. Aircr.* **1987**, *24*, 629–637. [[CrossRef](#)]
48. Bak, C.; Gaunaa, M.; Andersen, P.B.; Buhl, T.; Hansen, P.; Clemmensen, K. Wind tunnel test on airfoil Risø-B1-18 with an Active Trailing Edge Flap. *Wind Energy* **2010**, *13*, 207–219. [[CrossRef](#)]
49. Sven Geisbauer, T.L. Towards the Investigation of Unsteady Spoiler Aerodynamics. In Proceedings of the 35th AIAA Applied Aerodynamics Conference, Denver, CO, USA, 5–9 June 2017. A.A. Forum.
50. Mack, M.D.; Seetharam, H.D.; Kuhn, W.G.; Bright, J.T. Aerodynamics of Spoiler Control Devices. In Proceedings of the AIAA Aircraft Systems and Technology Meeting, New York, NY, USA, 20–22 August 1979. A.P. 1979-1873.
51. Wentz, J.W.; Ostowari, C.; Seetharam, H.C. Effects of Design Variables on Spoiler Control Effectiveness, Hinge Moments and Wake Turbulence. In Proceedings of the 19th AIAA Aerospace Sciences Meeting, Louis, MO, USA, 12–15 January 1981. AIAA Paper 1981-0072.
52. Maskell, E.C. *Pressure Distributions Illustrating Flow Reattachment behind a Forward Mounted Flap*; ARC-CP-211; Her Majesty's Stationery Office: London, UK, 1955.
53. Croom, D.R.; Shufflebarger, C.C.; Huffman, J.K. *An Investigation of Forward-Located Fixed Spoilers and Deflectors as Gust Alleviators on an Unswept-Wing Model*; NACA-TN-3705; NACA: Boston, MA, USA, 1956.
54. Siddalingappa, S.R.; Hancock, G.J. *An Introduction to the Aerodynamics of Spoilers*; Paper QMC EP-1034; Department of Aeronautical Engineering, Queen Mary College: London, UK, 1980.
55. Mabey, D.G. Experimental Methods to Determine Control Effectiveness in Wind Tunnels. In *AGARD Special Course on Aerodynamic Characteristics of Controls*; AGARD-R-711 Paper 5; AGARD: Neuilly sur Seine, France, July 1995.
56. Hancock, G.J. Dynamic Effects of Controls. In *AGARD Special Course on Aerodynamic Characteristics of Controls*; AGARD-R-711 Paper 4; AGARD: Neuilly sur Seine, France, July 1995.
57. Consigny, H.; Gravelle, A.; Molinaro, R. Aerodynamic Characteristics of a Moving Two-Dimensional Spoiler in Subsonic and Transonic Flow. *J. Aircr.* **1984**, *21*, 683–687. [[CrossRef](#)]
58. Kalligas, K. The Dynamic Characteristics of Two-Dimensional Spoilers at Low Speeds. Ph.D. Thesis, Department of Aeronautical Engineering, University of Bristol, Bristol, UK, 1986.
59. Nelson, C.F.; Koga, D.J.; Eaton, J.K. Unsteady, Separated Flow Behind an Oscillating, Two-Dimensional Spoiler. *AIAA J.* **1990**, *28*, 845–852. [[CrossRef](#)]
60. Mineck, R.E. Reynolds Number Effects on the Performance of Ailerons and Spoilers. In Proceedings of the 39th AIAA Aerospace Sciences Meeting and Exhibit, Reno, NV, USA, 8–11 January 2001. AIAA Paper 2001-0908.
61. Geisbauer, S. Numerical Simulation and Validation of Aerodynamics of Static and Dynamic Spoilers. *J. Aircr.* **2021**, *58*, 1187–1203. [[CrossRef](#)]
62. Roth, D.; Enenkl, B.; Dieterich, O. Active rotor control by flaps for vibration reduction—Full scale demonstrator and first flight test results. In Proceedings of the 32nd European Rotorcraft Forum, Maastricht, The Netherlands, 12–14 September 2006.

63. Kota, S.; Hetrick, J.A.; Osborn, R.; Paul, D.; Pendleton, E.; Flick, P.; Tilmann, C. Design and application of compliant mechanisms for morphing aircraft structures. In Proceedings of the SPIE, San Diego, CA, USA, 4–5 August 2003; pp. 24–33.
64. Buhl, T.; Gaunaa, M.; Bak, C. Potential Load Reduction Using Airfoils with Variable Trailing Edge Geometry. *J. Sol. Energy Eng.* **2005**, *127*, 503–516. [[CrossRef](#)]
65. Chow, R.; Dam, C.P.V. Unsteady Computational Investigations of Deploying Load Control Microtabs. *J. Aircr.* **2006**, *43*, 1458–1469. [[CrossRef](#)]
66. Blaylock, M.; Chow, R.; van Dam, C.P. Comparison of Microjets with Microtabs for Active Aerodynamic Load Control. In Proceedings of the 5th Flow Control Conference, Chicago, IL, USA, 28 June–1 July 2010. AIAA 2010-4409.
67. Johnson, S.J.; Baker, J.P.; Van Dam, C.P.; Berg, D. An overview of active load control techniques for wind turbines with an emphasis on microtabs. *Wind Energy* **2010**, *13*, 239–253. [[CrossRef](#)]
68. Van Dam, C.P.; Berg, D.E.; Johnson, S.J. *Active Load Control Techniques for Wind Turbines*; SAND2008-4809; Sandia National Laboratories (SNL): Albuquerque, NM, USA; Livermore, CA, USA, 2008.
69. Guo, S.; Jing, Z.W.; Li, H.; Lei, W.T.; He, Y.Y. Gust response and body freedom flutter of a flying-wing aircraft with a passive gust alleviation device. *Aerosp. Sci. Technol.* **2017**, *70*, 277–285. [[CrossRef](#)]
70. Castrichini, A.; Siddaramaiah, V.H.; Calderon, D.E.; Cooper, J.E.; Wilson, T.; Lemmens, Y. Preliminary investigation of use of flexible folding wing tips for static and dynamic load alleviation. *Aeronaut. J.* **2017**, *121*, 73–94. [[CrossRef](#)]
71. Castrichini, A.; Cooper, J.E.; Wilson, T.; Carrella, A.; Lemmens, Y. Nonlinear Negative Stiffness Wingtip Spring Device for Gust Loads Alleviation. *J. Aircr.* **2017**, *54*, 627–641. [[CrossRef](#)]
72. Castrichini, A.; Siddaramaiah, V.; Calderon, D.; Cooper, J.; Wilson, T.; Lemmens, Y. Nonlinear Folding Wing Tips for Gust Loads Alleviation. *J. Aircr.* **2016**, *53*, 1391–1399. [[CrossRef](#)]
73. Chan, D.T.; Jones, G.S.; Milholen, W.E.; Goodliff, S.L. Transonic Drag Reduction Through Trailing-Edge Blowing on the FAST-MAC Circulation Control Model. In Proceedings of the 35th AIAA Applied Aerodynamics Conference, Denver, CO, USA, 5–9 June 2017. AIAA AVIATION Forum, AIAA 2017-3246.
74. Cui, W.; Zhu, H.; Xia, C.; Yang, Z. Comparison of Steady Blowing and Synthetic Jets for Aerodynamic Drag Reduction of a Simplified Vehicle. *Procedia Eng.* **2015**, *126*, 388–392. [[CrossRef](#)]
75. Zahn, J.; Rist, U. Active and Natural Suction at Forward-Facing Steps for Delaying Laminar–Turbulent Transition. *AIAA J.* **2017**, *55*, 1343–1354. [[CrossRef](#)]
76. Guo, Z.; Kloker, M.J. Control of crossflow-vortex-induced transition by unsteady control vortices. *J. Fluid Mech.* **2019**, *871*, 427–449. [[CrossRef](#)]
77. Zhang, H.; Chen, S.; Meng, Q.; Wang, S. Flow separation control using unsteady pulsed suction through endwall bleeding holes in a highly loaded compressor cascade. *Aerosp. Sci. Technol.* **2018**, *72*, 455–464. [[CrossRef](#)]
78. Greenblatt, D.; Wagnanski, I.J. The control of flow separation by periodic excitation. *Prog. Aerosp. Sci.* **2000**, *36*, 487–545. [[CrossRef](#)]
79. Paul, A.R.; Joshi, S.; Jindal, A.; Maurya, S.P.; Jain, A. Experimental Studies of Active and Passive Flow Control Techniques Applied in a Twin Air-Intake. *Sci. World J.* **2013**, *2013*, 1–8. [[CrossRef](#)] [[PubMed](#)]
80. Paul, A.R.; Kuppa, K.; Yadav, M.S.; Dutta, U. Flow Improvement in Rectangular Air Intake by Submerged Vortex Generators. *J. Appl. Fluid Mech.* **2011**, *4*, 77–86.
81. Ebrahimi, A.; Hajipour, M.; Ghamkhar, K. Experimental study of stall control over an airfoil with dual excitation of separated shear layers. *Aerosp. Sci. Technol.* **2018**, *82–83*, 402–411. [[CrossRef](#)]
82. Amitay, M.; Glezer, A. Role of Actuation Frequency in Controlled Flow Reattachment over a Stalled Airfoil. *AIAA J.* **2002**, *40*, 209–216. [[CrossRef](#)]
83. Korbacher, G.K.; Sridhar, K. *A Review of the Jet Flap*; UTIA Review, No. 14; University of Toronto Press: Toronto, ON, CA, 1960.
84. Traub, L.W.; Miller, A.C.; Rediniotis, O. Comparisons of a Gurney and Jet-Flap for Hinge-Less Control. *J. Aircr.* **2004**, *41*, 420–423. [[CrossRef](#)]
85. Blaylock, M.; Chow, R.; Cooperman, A.; Dam, C.P. Comparison of pneumatic jets and tabs for Active Aerodynamic Load Control. *Wind Energy* **2014**, *17*, 1365–1384. [[CrossRef](#)]
86. Rao, P.; Strganac, T.; Rediniotis, O. Control of aeroelastic response via synthetic jet actuators. In Proceedings of the 41st Structures, Structural Dynamics, and Materials Conference and Exhibit, Atlanta, GA, USA, 3 April 2000; American Institute of Aeronautics and Astronautics: Reston, VA, USA, 2000. [[CrossRef](#)]
87. De Breuker, R.; Abdalla, M.; Marzocca, P.; Gürdal, Z. Flutter suppression using synthetic jet actuators: The typical section. In Proceedings of the 17th International Conference on Adaptive Structures and Technologies, Taipei, Taiwan, 16–19 October 2006; pp. 402–409.
88. De Vries, H.; Boeije, C.; Cleine, I.; van Emden, E.; Zwart, G.; Stobbe, H.; Hirschberg, A.; Hoeijmakers, H. Fluidic Load Control for Wind Turbine Blades. In Proceedings of the 47th AIAA Aerospace Sciences Meeting including the New Horizons Forum and Aerospace Exposition, Orlando, FL, USA, 5 January 2009. AIAA 2009-684. [[CrossRef](#)]
89. Heathcote, D.; Al-Battal, N.; Gursul, I.; Cleaver, D. Control of Wing Loads by Means of Blowing and Mini-Tabs. In Proceedings of the European Drag Reduction and Flow Control Meeting—EDRFCM 2015, Cambridge, UK, 23–26 March 2015.
90. Lockwood, V.E.; Vogler, R.D. *Exploratory Wind-Tunnel Investigation at High Subsonic and Transonic Speeds of Jet Flaps on Unswept Rectangular Wings*; NACA-TN-4353; NACA: Boston, MA, USA, 1958.

91. Mikolowsky, W.; McMahon, H. An Experimental Investigation of a Jet Issuing from a Wing in Crossflow. *J. Aircr.* **1973**, *10*, 546–553. [[CrossRef](#)]
92. Li, Y.; Qin, N. Gust load alleviation by normal microjet. *Aerosp. Sci. Technol.* **2021**, *117*, 106919. [[CrossRef](#)]
93. Al-Battal, N.H.; Cleaver, D.J.; Gursul, I. Unsteady actuation of counter-flowing wall jets for gust load attenuation. *Aerosp. Sci. Technol.* **2019**, *89*, 175–191. [[CrossRef](#)]
94. Mueller-Vahl, H.; Nayeri, C.; Paschereit, C.O.; Greenblatt, D. Control of Unsteady Aerodynamic Loads Using Adaptive Blowing. In Proceedings of the 32nd AIAA Applied Aerodynamics Conference, Atlanta, GA, USA, 16–20 June 2014.
95. De Breuker, R.; Abdalla, M.; Marzocca, P. Aeroelastic Control and Load Alleviation using Optimally Distributed Synthetic Jet Actuators. In Proceedings of the 48th AIAA/ASME/ASCE/AHS/ASC Structures, Structural Dynamics, and Materials Conference, Honolulu, Hawaii, 23 April 2007; American Institute of Aeronautics and Astronautics: Reston, VA, USA, 2007. [[CrossRef](#)]
96. Alexander, M.G.; Anders, S.G.; Johnson, S.K.; Florance, J.P.; Keller, D.F. *Trailing Edge Blowing on a Two-Dimensional Six-Percent Thick Elliptical Circulation Control Airfoil up to Transonic Conditions*; NASA/TM-2005-213545; Sponsoring Organization; NASA Langley Research Center: Hampton, VA, USA, 2005.
97. Ahuja, K.; Sankar, L.; Englar, R.J.; Munro, S.; Liu, Y. *Application of Circulation Control Technology to Airframe Noise Reduction*; GIT. Annual Performance Report; Georgia Institute of Technology: Atlanta, GA, USA, 2000; Volume 5928, pp. 1–2146.
98. Nichols, J.H.; Englar, R.J. Advanced circulation control wing system for navy stol aircraft. *J. Aircr.* **1981**, *18*, 1044–1050. [[CrossRef](#)]
99. Cook, M.V.; Buonanno, A.; Erbslöh, S.D. A circulation control actuator for flapless flight control. *Aeronaut. J.* **2008**, *112*, 483–489. [[CrossRef](#)]
100. Englar, R.; Smith, M.; Kelley, S. Application of circulation control to advanced subsonic transport aircraft. I—Airfoil development. II—Transport application. *J. Aircr.* **1994**, *31*, 1160–1177. [[CrossRef](#)]
101. Crowther, W.; Wilde, P.; Gill, K.; Michie, S.M. Towards Integrated design of fluidic flight controls for a flapless aircraft. *Aeronaut. J.* **2009**, *113*, 699–713. [[CrossRef](#)]
102. John, P. The flapless air vehicle integrated industrial research (FLAVIIR) programme in aeronautical engineering. *Proc. Inst. Mech. Eng. Part G J. Aerosp. Eng.* **2010**, *224*, 355–363. [[CrossRef](#)]
103. Wilde, P.; Buonanno, A.; Crowther, W.; Savvaris, A. Aircraft control using fluidic maneuver effectors. In Proceedings of the 26th AIAA Applied Aerodynamics Conference, Honolulu, Hawaii, 18–21 August 2008. AIAA 2008-6406.
104. Hoholis, G.; Steijl, R.; Badcock, K. Circulation Control as a Roll Effector for Unmanned Combat Aerial Vehicles. *J. Aircr.* **2016**, *53*, 1875–1889. [[CrossRef](#)]
105. Wilde, P.I.A.; Crowther, W.J.; Harley, C.D. Application of circulation control for three-axis control of a tailless flight vehicle. *Proc. Inst. Mech. Eng. Part G J. Aerosp. Eng.* **2010**, *224*, 373–386. [[CrossRef](#)]
106. Li, Y.; Qin, N. Airfoil gust load alleviation by circulation control. *Aerosp. Sci. Technol.* **2020**, *98*, 105622. [[CrossRef](#)]
107. Li, Y.; Qin, N. Gust load alleviation on an aircraft wing by trailing edge Circulation Control. *J. Fluids Struct.* **2021**, *107*, 103407. [[CrossRef](#)]